Heat Transfer in Rotating Serpentine Passages with Smooth Walls

J. H. WAGNER
United Technologies Research Center
East Hartford, CT 06108

B. V. JOHNSON
United Technologies Research Center
East Hartford, CT 06108

F. C. KOPPER
Pratt and Whitney
Commercial Engine Business
East Hartford, CT 06108

ABSTRACT

Experiments were conducted to determine the effects of buoyancy and Coriolis forces on heat transfer in turbine blade internal coolant passages. The experiments were conducted with a large scale, multi–pass, smooth–wall heat transfer model with both radially inward and outward flow. An analysis of the governing flow equations showed that four parameters influence the heat transfer in rotating passages (coolant–to–wall temperature ratio, Rossby number, Reynolds number and radius–to–passage hydraulic diameter ratio). These four parameters were varied over ranges which are typical of advanced gas turbine engine operating conditions. It was found that both Coriolis and buoyancy effects must be considered in turbine blade cooling designs and that the effect of rotation on the heat transfer coefficients was markedly different depending on the flow direction. Local heat transfer coefficients were found to decrease by as much as 60 percent and increase by 250 percent from no rotation levels. Comparisons with a pioneering stationary vertical tube buoyancy experiment showed reasonably good agreement. Correlation of the data is achieved employing dimensionless parameters derived from the governing flow equations.

NOMENCLATURE

A	Area of passage cross–section
D	Hydraulic diameter
Gr	Rotational Grashof number
h	Heat transfer coefficient
k	Thermal conductivity
m	Mass flowrate
Nu	Nusselt number, $h*D/k$
Pr	Prandtl number
R	Radius
Re	Reynolds number, $m*D/\mu/A$
Ro	Rotation number, $\Omega*D/V$
T	Temperature
V	Mean coolant velocity
x	Streamwise Distance
$\Delta\rho/\rho$	Density ratio, $(\rho_b - \rho_w)/\rho_b$
Ω	Rotational speed
ρ	Coolant density
μ	Absolute viscosity

Subscripts:

b	Bulk property
f	Film property
in	Inlet to model
w	Heated surface location
x	Based on streamwise location
∞	Fully developed, smooth tube

Superscripts:

–	Average

INTRODUCTION

In advanced gas turbine engines, increased temperatures, stage pressure ratios and rotor speeds are used to increase thrust/weight ratios and reduce the specific fuel consumption. Hence, the turbine blades are subjected to increased external gas path heat loads in addition to increased levels of stress. Efficient internal convection cooling is essential to achieving good fuel consumption and acceptable blade life. Knowledge of the local heat transfer in the cooling passages is extremely important in the prediction of blade metal temperatures, i.e. blade life. Rotation of turbine blade cooling passages gives rise to Coriolis and buoyancy forces which can significantly alter the local heat transfer in the internal coolant passages from the development of cross stream (Coriolis), as well as,

radial (buoyant) secondary flows. Buoyancy forces in gas turbine blades are substantial because of the high rotational speeds and coolant temperature gradients. Earlier investigations (e.g. Eckert et al., 1953) with single pass co– and counter–flowing stationary coolant passages indicated that there can also be substantial differences in the heat transfer when the buoyancy forces are aligned with or counter to the forced convection direction. A better understanding of Coriolis and buoyancy effects and the capability to predict the heat transfer response to these effects will allow the turbine blade designer to achieve cooling configurations which utilize less flow and which reduce thermal stresses in the airfoil.

The complex coupling of the Coriolis and buoyancy forces has prompted many investigators to study the flow field generated in unheated, rotating circular and rectangular passages without the added complexity of buoyancy (Hart (1971), Wagner and Velkoff (1972), Moore (1967) and Johnston et al. (1972), Roth and Johnston (1979)). These investigators have documented strong secondary flows and have identified aspects of flow stability which produce streamwise oriented, vortexlike structures in the flow of rotating radial passages.

The effects of buoyancy on heat transfer without the complicating effects of Coriolis generated secondary flow have been studied in vertical stationary ducts. Effects of buoyancy on heat transfer were reported by Eckert et al. (1953), Metais and Eckert (1964) and Brundrett and Burroughs (1967). Flow criteria for forced–, mixed– and free–convection heat transfer was developed for parallel flow and counter flow configurations by Eckert et al. (1953) and Metais and Eckert (1964). Based on these experimental results, buoyancy forces would be expected to cause significant changes in the heat transfer in turbine blade coolant passages and be strongly dependent on flow direction (radially inward vs. radially outward).

The combined effects of Coriolis and buoyancy forces on heat transfer has been studied by a number of investigators. Heat transfer in rotating, smooth–wall models has been investigated by Guidez (1988) and Clifford (1985), Iskakov and Trushin (1983), Morris (1981), Morris and Ayhan (1979), Lokai and Gunchenko (1979), Johnson (1978), and Mori et al. (1971). Large increases and decreases in local heat transfer were found to occur by some investigators under certain conditions of rotation while others showed lesser effects. Analysis of these results do not show consistent trends. The inconsistency of the previous results is attributed to differences in the measurement techniques, models and test conditions.

A comprehensive experimental program was formulated to identify and separate effects of Coriolis and buoyancy for the range dimensionless flow parameters encountered in axial flow, aircraft gas turbines. The overall objective of this experimental program was to acquire and correlate benchmark–quality heat transfer data for a multi–pass, coolant passage under conditions similar to those experienced in the blades of advanced aircraft gas turbines. Heat transfer results were obtained under varying conditions of flowrate, rotation, model radius and wall–to–coolant temperature difference. The experiments were conducted by varying each parameter while holding the remaining parameters constant. The data was analyzed to separate the effects of Reynolds number, Coriolis forces, buoyancy,

streamwise location, flow direction and geometric location in the coolant passage (i.e., leading or trailing surfaces).

The results presented in this paper are from the first phase of a three phase program directed at studying the effects of rotation on a multi–pass model with smooth and rough wall configurations. The first phase utilized the smooth wall configuration. Subsequent phases to be reported in the future include surface roughness elements oriented at 90 and 45 degrees to the flow direction. Local heat transfer results were obtained along the smooth–wall coolant passage and around its periphery for radial outflow and inflow conditions. This paper presents heat transfer results obtained in the first, second and third radial passages of a multi–pass, smooth wall, square passage model. The results for outward flow in the first passage were previously presented by Wagner, Johnson and Hajek (1989). The flow direction in the first and third passage was radially outward. The flow direction of the connecting second passage was radially inward. The effect of flow direction on heat transfer in rotating coolant passages is the main focus of this paper. The results will show that significant differences occur in the heat transfer depending on flow direction and surface location. A paper with a more comprehensive discussion of the heat transfer in the turn regions is forthcoming and will be published after additional analysis.

The facility, data acquisition and data reduction techniques employed in this experiment were discussed in the Wagner et al. (1989) paper and will not be repeated. However, the description of the model will be repeated for the ease of the reader.

DESCRIPTION OF EXPERIMENTAL EQUIPMENT

Heat Transfer Model

The heat transfer model was designed to simulate the internal multi–passage geometry of a cooled turbine blade (Figure 1a). The model consists of three straight sections and three turn sections which were instrumented followed by one uninstrumented straight section, as shown in Figure 1b. Data presented herein were obtained in the first, second and third passages with radially outward, inward and outward flow, respectively. The model passages are square with a sidewall dimension of 0.5 in. (12.7 mm). The heated length of the first passage is 14 hydraulic diameters and is comprised of sixteen heated copper elements at four streamwise locations. Four elements form the walls of the square coolant passage at each streamwise location. The two cross–section views shown in the figure show the orientation of the leading, trailing and sidewall surfaces. Each copper element is heated on the side opposite the test surface with a thin film, 0.003 in. (0.1 mm), resistance heater. Each element is 0.150 in. (3.8 mm) thick and is thermally isolated from surrounding elements by 0.060 in. (1.5 mm) thick fiberglass insulators. The insulating material separating the copper elements at each streamwise location resulted in a 0.04 in. (1.0 mm) chamfer in the corners, which yielded a hydraulic diameter in the straight sections of 0.518 in. (13.2 mm). The power to each element was adjusted to obtain an isothermal wall boundary condition. In practice, temperature gradients less than 2F (1C) were achieved. The heat flux between elements with a 2F (1C)
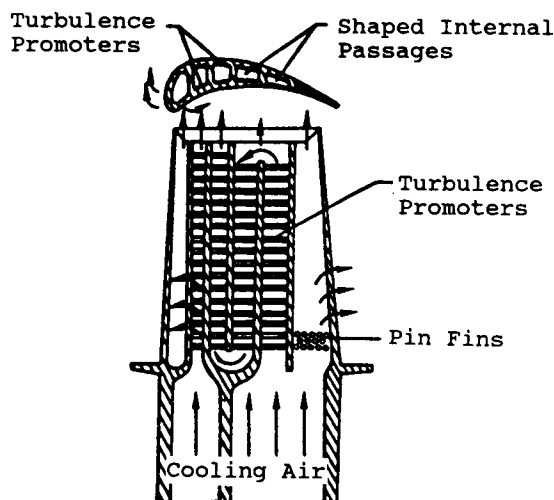
Fig. 1a   Typical Turbine Blade Internal
          Convection Cooling Configuration
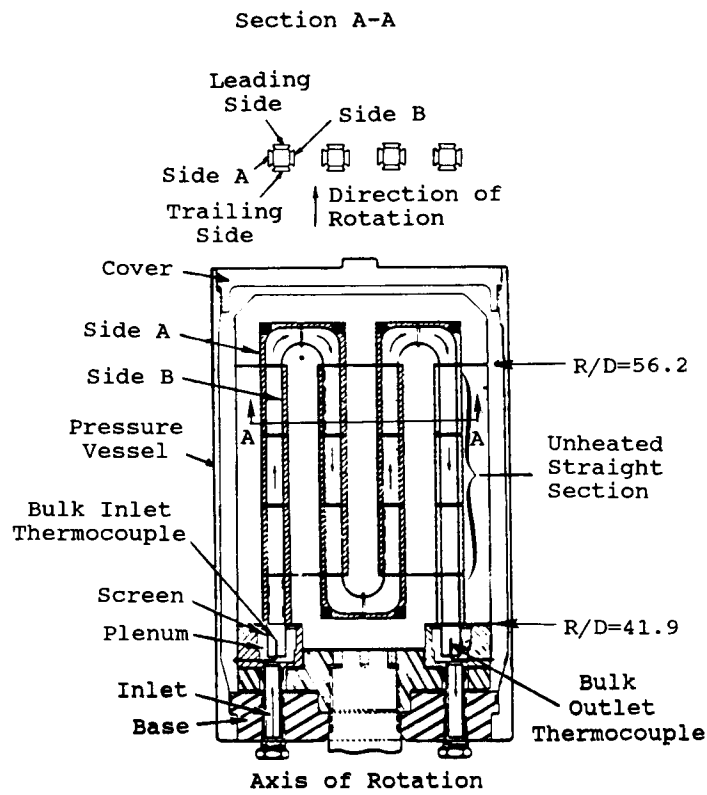   (from Han et. al. [1984])

Fig. 1b   Cross Sectional Views of Coolant
          Passage Heat Transfer Model
          Assembly

temperature difference was estimated to be less than 2 percent of a typical stationary heat flux.

Testing was conducted with air at nondimensional flow conditions typical of advanced gas turbine designs. The required

dimensionless rotation numbers were obtained with rotation rates of 1100 RPM or less by operating the model at a pressure of approximately 10 atmospheres. The model inlet air temperature was typically 80F (27C) and the copper elements were held at 120F, 160F, 200F and 240F (49C, 71C, 93C and 116C) for coolant–to–wall temperature differences of 40F, 80F, 120F and 160F (22C, 44C, 67C and 89C). Temperatures of the copper elements were measured with two chromel–alumel thermocouples inserted in drilled holes of each element. Heat transfer coefficients were determined by performing an energy balance on each copper element to obtain the convected heat flux and the local coolant temperature. See Wagner et al. (1989) for additional information about the data reduction procedure.

Nusselt numbers and Reynolds numbers were calculated for each element. The fluid properties in the Nusselt and Reynolds numbers were evaluated at the film temperature, i.e., $T_f = (T_w - T_b)/2$. All of the heat transfer results presented herein have been normalized with a smooth tube correlation for fully developed, turbulent flow. The constant heat flux Colburn equation, adjusted for constant wall temperature was used to obtain the Nusselt number for fully developed, turbulent flow in a smooth tube (Kays and Perkins (1973)). The resulting equation for the constant wall temperature condition with a Prandtl number equal to 0.72 is as follows.

$$Nu_\infty = 0.0176\ Re^{0.8}$$

An uncertainty analysis of the data reduction equations showed that approximately 3/4 of the estimated uncertainty in calculating heat transfer coefficient was due to the measurement of temperature in the model. The uncertainty of the heat transfer coefficient is influenced mainly by the wall–to–coolant temperature difference and the net heat flux from each element. Uncertainty in the heat transfer coefficient increases when either the temperature difference or the net heat flux decreases. For increasing x/D, the uncertainty increases because the wall–to–coolant temperature difference decreases. For low heat fluxes (i.e. low Reynolds numbers and on leading surfaces with rotation) the uncertainty in the heat transfer increased. Estimates of the error in calculating heat transfer coefficient typically varied from approximately ±6 percent at the inlet to ±20 percent at the exit of the heat transfer model for the baseline test conditions. The uncertainty in the lowest heat transfer coefficient on the leading side of the third passage with rotation is estimated to be 30 percent.

RESULTS

Forward

Heat transfer in stationary experiments with smooth passages is primarily a function of the Reynolds number (a flow parameter) and the streamwise distance from the inlet, x/D (a geometric parameter). However, when rotation is applied, the heat transfer is also strongly influenced by the coupled effects of Coriolis and buoyancy and becomes asymmetric around the passage. An unpublished analysis of the equations of motion by Suo (1980), similar to that of Guidez (1988), showed that the basic dimensionless fluid dynamic parameters governing the flow in a radial coolant passage were the Reynolds number, the rotation number, $\Omega D/V$, the fluid density ratio,

$\Delta\rho/\rho$, and the geometric parameter, R/D. Note that the rotation parameter is the reciprocal of the Rossby number, $V/\Omega D$, and governs the formation of cross–stream secondary flow. The rotation number, $\Omega D/V$, the fluid density ratio, $\Delta\rho/\rho$, and the geometric parameter, R/D, appear in the governing equation as a buoyancy parameter. This buoyancy parameter, $(\Delta\rho/\rho)$ $(R/D)(\Omega D/V)^2$, is the equivalent of Gr/Re^2 for stationary heat transfer. Thus, with rotation, the heat transfer is primarily a function of two geometric parameters (x/D and surface orientation relative to the direction of rotation) and three flow parameters (Reynolds number, rotation number and the buoyancy parameter).

Due to the vector nature of the equations of motion, it can also be expected that flow direction can also have a significant effect on the coolant flow. In the parallel flow case the flow is radially inward, coincident with buoyancy driven flow for heated walls. For the counter–flow case the flow is radially outward, opposite to the direction of the buoyancy driven flow. Flow direction (i.e. radially inward or outward) and a fixed radially outward directed force field, created by the rotating reference frame, establish the potential for parallel and counter flow situations as observed by Eckert et al. (1953) in their vertical tube experiment.

The format of this paper is to show the effects of each of the primary variables (x/D, rotation number, density ratio) on the heat transfer about a baseline flow condition to develop an understanding of the cause/effect relationships. The entire body of experimental results are then examined to determine the effect of the buoyancy parameter on the heat transfer for certain locations in the coolant passage.

Baseline Experiments

Two baseline experiments, one stationary and one rotating, were conducted to obtain data for comparison with all other data generated in this program. The stationary and rotating baseline experiments had dimensionless flow conditions which consisted of a Reynolds number of 25,000 and an inlet density ratio, $(\Delta\rho/\rho)_i = (T_w-T_b)/T_w$, of 0.13. The rotating baseline experiment had a rotation number, $\Omega D/V$, of 0.24 and a radius ratio at the average model radius, R/D, of 49. These values were selected because they are in the central region of the operating range of current large aircraft gas turbine engines.

Stationary. Streamwise variations of Nusselt number for the stationary baseline test are shown in Figure 2. The Nusselt number for fully developed, turbulent flow in a smooth tube with constant wall temperature is shown for comparison. In general, the heat transfer decreases in all three instrumented passages by about 25 percent from the first to the last heat transfer element of each straight section.

From Figure 2 it can also be seen that the heat transfer in the turn sections increases by a factor of approximately two compared to the fully developed, smooth passage heat transfer value. The heat transfer on the sidewall elements is complex and is indicative of heat transfer caused by a highly three dimensional flowfield.

Re $\approx$ 25,000 (Baseline)
$\Delta T \approx 80^{\circ}F$ (Baseline)

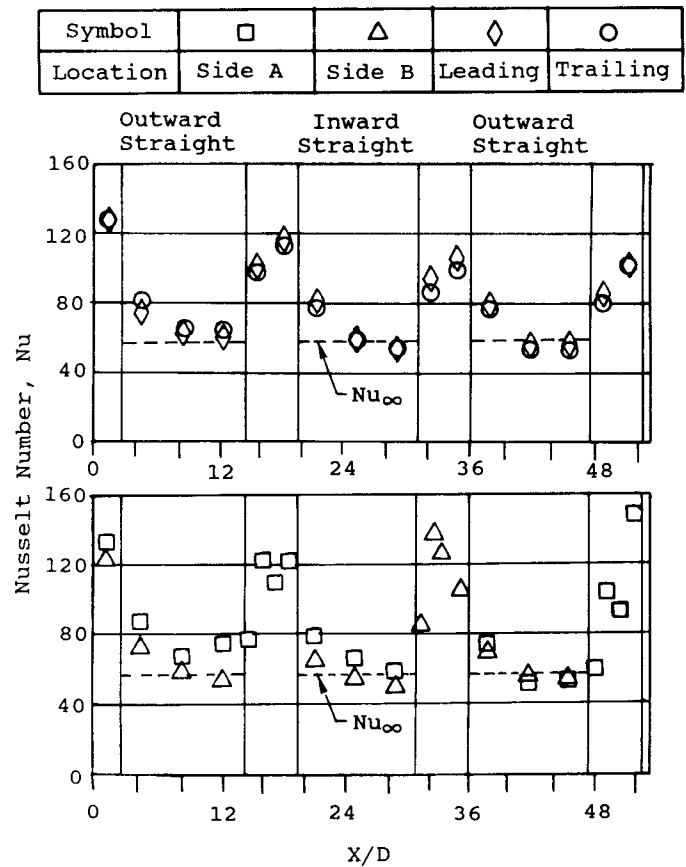| Symbol	□	△	◇	○
Location	Side A	Side B	Leading	Trailing

Fig. 2 Heat Transfer Results for Stationary Flow Condition

The streamwise distributions of the average heat transfer ratio for the stationary baseline experiment is shown in Figure 3 for the first two heated straight sections. The wall–to–wall variation of the heat transfer results from the four surfaces around the circumference of each coolant passage are also shown. Results from other investigators (Boelter et al., 1948, Aladyev, 1954, and Yang and Liao, 1973) are shown for comparison.

The streamwise variations in average heat transfer ratio for each passage are indicative of developing flow in the entrance region of a passage. Heat transfer ratio decreases with increasing streamwise location, x/D, to about 1.0 near the exit of each passage. A heat transfer ratio of 1.0 is that expected for fully developed, turbulent flow with a constant wall temperature. Although the mean inlet velocity profiles for the first passage were conditioned to be hydrodynamically "fully developed," it would be expected that the streamwise variation in heat transfer would be similar to that in a duct with an unheated starting length. This is evident in the data. The heat transfer distributions in the second and third passages also indicate that a development process occurs which is attributed to secondary flow effects of the turn. The wall–to–wall variations in heat transfer ratio for each streamwise location is less than 15 percent, indicating good passage symmetry.
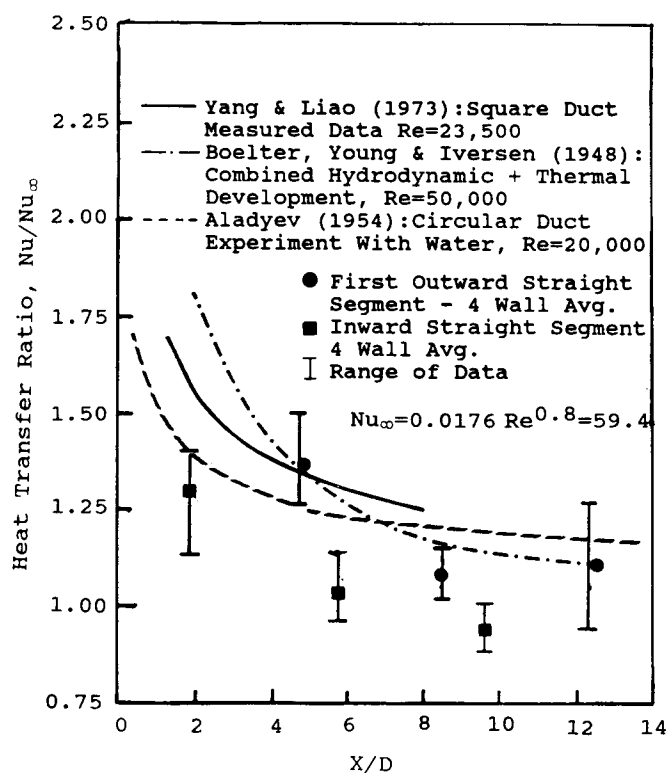
4

Fig. 3   Comparison of Heat Transfer Results in Straight Passages for the Stationary Flow Condition with Previous Entrance Region Heat Transfer Results

Fig. 4   Variation of Heat Transfer Ratio with Streamwise Location for "Rotating" Baseline Flow Condition; Re=25000, R_o=0.24, $(\Delta\rho/\rho)_i$=0.13

Rotating. The streamwise distributions of heat transfer ratio for the rotating baseline condition for the first two coolant passages are shown in Figure 4. The streamwise distributions of heat transfer ratio from the stationary baseline test are also shown. With rotation, heat transfer increases and decreases by factors of more than two from the trailing and leading surfaces, respectively, compared to the heat transfer from the stationary baseline test. The heat transfer from the sidewall surfaces increases by 20 to 50 percent. Note that the local heat transfer ratio on the leading side of the first coolant passage decreases rapidly with increasing streamwise distance to about 40 percent of the stationary value at x/D = 8.5 and then increases at the larger x/D location. The heat transfer ratio on the trailing side of this passage increases with increasing streamwise distance to almost 2.5 times that of a fully developed, smooth tube. This results in a 5–to–1 ratio of the heat transfer coefficients between the trailing and leading surfaces.

The effect of rotation on the heat transfer in the second, inward flowing passage is significantly different compared to that in the first, outward flowing passage. The heat transfer increases only about 10 to 20 percent on the leading surfaces compared to the stationary results. The heat transfer on the trailing surfaces decreases by 5 to 30 percent compared to the stationary values. These modest changes in heat transfer on the leading and trailing surfaces in the second passage result in a substantially reduced leading–to–trailing surface heat transfer variation.
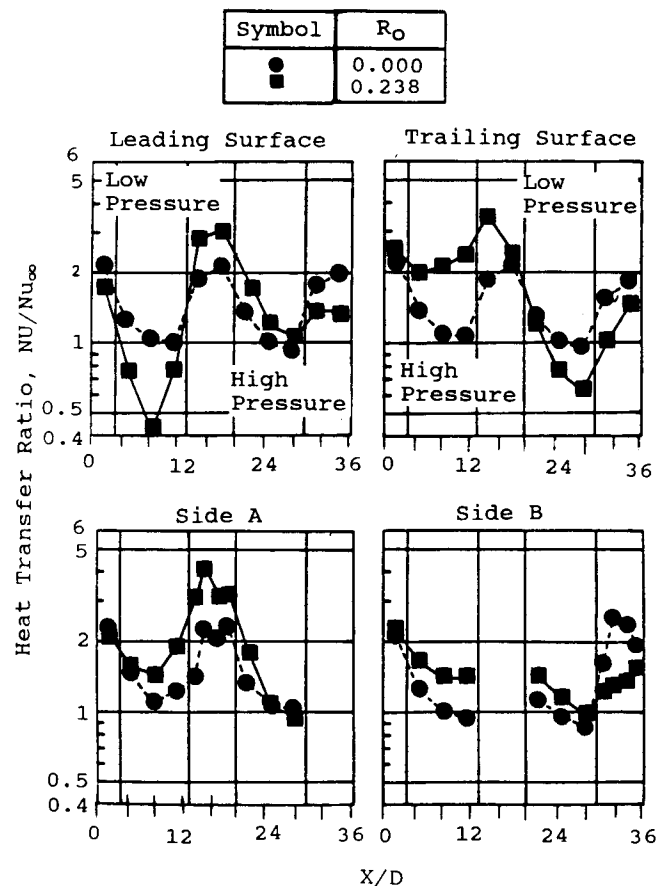
The effect of rotation on the heat transfer from the sidewall surfaces in the straight passages resulted in heat transfer increases which ranged from 0 to 50 percent.

A comprehensive discussion of the effects of rotation on heat transfer in the first passage was presented by Wagner et al. (1989). In summary, the difference in heat transfer between the rotating and nonrotating flow conditions is primarily attributed to the secondary flows associated with the Coriolis force and the buoyancy. The decrease in heat transfer near the inlet of the passage on the leading surfaces of the first passage was attributed to the stabilizing of the near–wall flow. The subsequent increase in heat transfer near the end of the first passage was postulated to occur when the passage secondary flows become more developed and interact with the buoyant, stabilized near–wall flow on the leading side of the passage.

The change in heat transfer due to rotation is somewhat different for the second, inward flowing passage, compared to the change observed in the first passage. For the inward flowing passage the heat transfer is expected to increase on the leading surfaces and decrease on the trailing surfaces, opposite to the effect noted in the first passage. Eckert et al. (1953) showed that average heat transfer was reduced in a stationary, parallel flow configuration, where the mean convective flow direction and the buoyancy induced flow direction

are the same (i.e., as in the second, inward flowing passage). The effects of rotation are in general agreement with the aforementioned discussions except that heat transfer did not decrease nearly as much on the trailing surfaces of the second passage compared to the leading surfaces of the first passage. Additionally, the large increases in heat transfer expected on leading surfaces of the second passage did not occur as they did on the trailing surfaces of the first passage.

The difference in the heat transfer on the high pressure sides of the coolant passage (i.e. trailing surfaces in the first, outward flowing passage and leading surfaces in the second, inward flowing passage) is believed to be a result of the combined effects of the formation of boundary layer vortices (Johnston et al. (1972) and Eckert et al. (1953)) and to counteracting buoyancy effects caused when the buoyancy force direction is aligned with the flow direction. When a counter flow situation exists (i.e. buoyancy opposite to that of flow direction), the combined effects of buoyant and Coriolis–driven secondary flows causes an increase in heat transfer. When a parallel situation exists (i.e. aligned buoyancy and flow direction) the combined effects are less because of a counteraction of the two flow mechanisms. Further discussion of these effects will be presented in subsequent sections.

The baseline results with rotation showed significant changes in the heat transfer in the first passage on the leading, trailing, and turn surfaces but relatively smaller changes on the sidewall surfaces. Therefore, the following discussion will focus on the heat transfer results from only the leading and trailing surfaces in the straight

sections of the coolant passage with both inward and outward flow and will focus on the differences between inward vs. outward flow. Discussion of effects of rotation on the heat transfer in the turn regions of the coolant passage are deferred to a subsequent paper.

Varying Rotation Number

The rotation number, $\Omega D/V$, was varied from 0 to 0.48 for this series of flow conditions. The Reynolds number, inlet density ratio and radius ratio were held constant at the nominal values of 25,000, 0.13 and 49, respectively.

High Pressure Surfaces. Increasing the rotation rate causes significant increases in heat transfer on the trailing surfaces (Figure 5a) of the first passage but lesser increases on the leading surfaces in the second passage (Figure 5b). Heat transfer in the first passage increased by more than a factor of 3.5 for the largest value of rotation parameter (0.48) compared to stationary heat transfer values. Compared to the stationary results, heat transfer on the leading, high pressure side of the second passage experienced modest increases of approximately 50 percent. The effects on heat transfer due to Coriolis generated secondary flows might be expected to be approximately the same for the first and second passages. The differences in heat transfer between the outward and inward flowing passages is therefore attributed to the different effects of buoyancy in the counter–flowing first passage (radially outward flow) and the co–flowing second passage (radially inward flow).
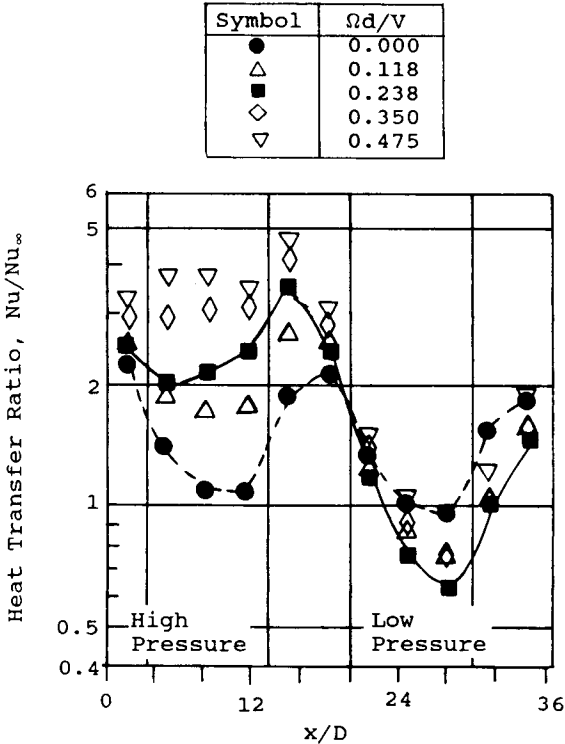
Symbol	$\Omega d/V$
●	0.000
△	0.118
■	0.238
◇	0.350
▽	0.475

Symbol	$\Omega d/V$
●	0.000
△	0.118
■	0.238
◇	0.350
▽	0.475

Fig. 5a   Effect of Rotation Number on Heat Transfer Ratio for Trailing Surfaces; Re=25000, $(\Delta \rho/\rho)_i$=0.13, R/D=49
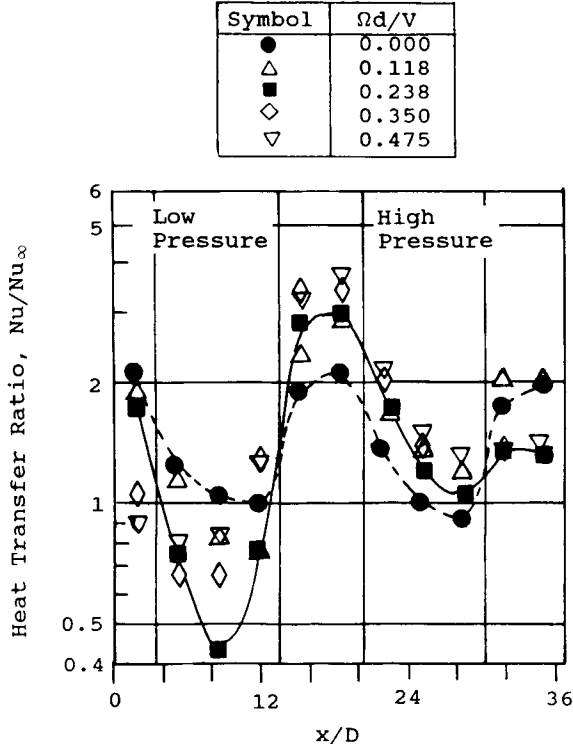

Fig. 5b   Effect of Rotation Number on Heat Transfer Ratio for Leading Surfaces; Re=25000, $(\Delta \rho/\rho)_i$=0.13, R/D=49

The lesser increases in the heat transfer ratio on the high pressure side of the second passage is attributed to a reduction in the generation of near–wall turbulence. In the first passage the near–wall buoyancy driven flow was inward toward the axis of rotation and the coolant flow was outward. This counter flow situation generated additional near–wall turbulence due to the strong shear gradient. This destabilizing of the shear flow combined with the cross stream secondary flows generated by Coriolis forces causes large increases in heat transfer in the first passage. However, when the flow and the buoyancy driven near–wall flows are coincident, as in the second passage, the generation of near–wall turbulence may be diminished because of the relatively weaker near–wall shear layer. Therefore, the combined effects of the buoyant and the cross stream secondary flows in the second passage on the heat transfer was less. The magnitude of the buoyancy effect on the heat transfer is unclear in that the buoyancy effect on the heat transfer in the second passage may be zero (which implies a modest Coriolis dominated heat transfer increase) or negative (which implies a larger Coriolis dominated heat transfer increase which is offset by a reduction due to buoyancy). Ongoing numerical simulations of these test points will help in the understanding of this complex flow field.

Low Pressure Surfaces. In contrast to the continual increase in heat transfer with increasing rotation number on the trailing side, the heat transfer ratio decreases with increasing rotation number on the leading side of the passage near the inlet. For all of the remaining locations on the leading side of the passage, the heat transfer ratio decreases and then increases again with increasing rotation number. Heat transfer from the trailing, low pressure surfaces of the second passage also had large decreases in heat transfer. Heat transfer in the second passage decreased to almost 60 percent of the stationary heat transfer levels compared to 40 percent in the first passage. In the second passage, the heat transfer decreased and then subsequently increased again as the rotation rate was increased.

The decreases in the heat transfer ratio are attributed, for the most part, to the cross–stream flow patterns as well as the stabilization of the near–wall flow on the leading side of the passage (Johnston et al. (1972)). The cross–stream flows cause heated, near–wall fluid from the trailing and sidewall surfaces to accumulate near the leading side of the coolant passage resulting in reduced heat transfer. In addition, the rotation stabilizes the shear layers along this wall and further reduces the turbulent transport of heat. The increase in the heat transfer ratio in the latter half of the coolant passage for the larger rotation numbers is attributed to the large scale development of the Coriolis generated secondary flow cells. Similar effects of rotation are noted for the low pressure surfaces in both the first and second passages, irrespective of flow direction. These results suggest that the heat transfer on low pressure surfaces is dominated by Coriolis generated cross–stream flows which cause a stabilization of the near–wall flows and that the heat transfer on the high pressure surfaces is affected by a combination of Coriolis and buoyant effects. Therefore, it can be expected that the correlations of local heat transfer data may be substantially different depending on local flow conditions (i.e. due to differing near–wall shear gradients).

Varying Density Ratio

The inlet density ratio, $(\Delta\rho/\rho)_i$, was varied from 0.07 to 0.22 for this series of flow conditions. The Reynolds number, rotation number and radius ratio were held constant at the baseline values of 25,000, 0.24 and 49, respectively. Heat transfer was obtained at a fixed rotation number and, therefore, conclusions can be obtained regarding the effects of buoyancy for flow conditions near the rotating baseline flow conditions.

Increasing the inlet density ratio (i.e., the wall–to–coolant temperature difference) from 0.07 to 0.22 causes the heat transfer ratio in the first passage to increase on all trailing surfaces by as much as 50 percent (Figure 6a) and on the leading surfaces by as much as 100 percent (Figure 6b). The exception to the general increase in heat transfer with increasing density ratio occurred near the inlet of the first passage on the leading side, where the heat transfer ratio is observed to decrease slightly.

Heat transfer in the second, inward flowing passage increases with increases in the temperature difference (Figure 6). In general, the increases in heat transfer in the second passage were approximately half of those in the first passage (on the order of 10 to 50 percent compared to maximum relative increase of 100 percent in the first passage). The differences in heat transfer behavior due to changes in the density ratio between the first and second passages are attributed to the differing mechanisms of Coriolis and buoyancy interaction. If the effect of Coriolis generated secondary flow on heat transfer is similar (regardless of flow direction) and the effect of density ratio for fixed rotation number generally causes heat transfer to increase, then the interaction of the two effects is significant and also counteracting. The counteraction of the two effects was deduced because of the relatively small increases in heat transfer on the high pressure side of the second passage.

Varying Rotation Number and Density Ratio

Additional data from parametric variations of density ratio and rotation parameter were necessary to isolate the effects of rotation and buoyancy. The inlet density ratio was varied from 0.07 to 0.22 for selected rotation numbers. Heat transfer results from these experiments were plotted vs. inlet density ratio with rotation number as a secondary variable. The distributions of heat transfer ratio with density ratio (not shown) were extrapolated for each value of the rotation number to obtain a value of the heat transfer ratio for a density ratio of 0.0 (i.e., limit as ΔT approaches 0.0). The heat transfer results obtained from the experiments plus the extrapolated values for a density ratio of 0.0 (dashed lines) are presented in Figure 7 as the variation of heat transfer ratio with the rotation number with the density ratio as the secondary variable for three streamwise locations for the first and the second passage. Heat transfer results in the first passage were thoroughly discussed by Wagner et al. (1989). Therefore, the following discussion will concentrate on the differences in the heat transfer from the first and second passages.

High Pressure Surfaces. Heat transfer results from the high pressure side of the first and second passages is shown in Figure 7 for ranges of rotation number and density ratio. Note that there is no
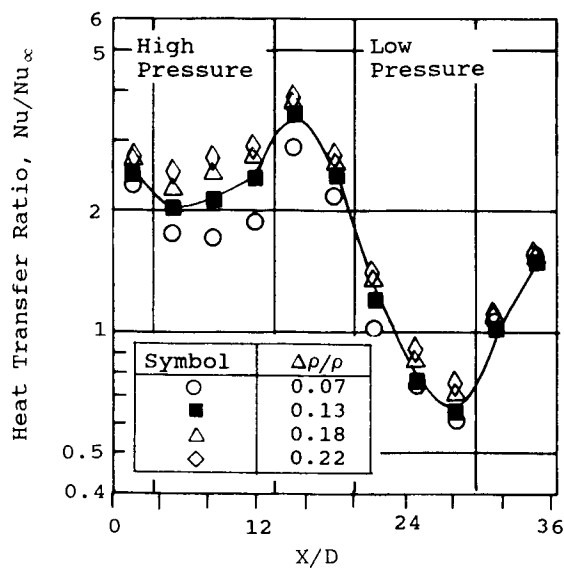
Fig. 6a   Effect of Wall-to-Coolant Density
          Difference on Heat Transfer Ratio
          for Trailing Surfaces; Re=25000,
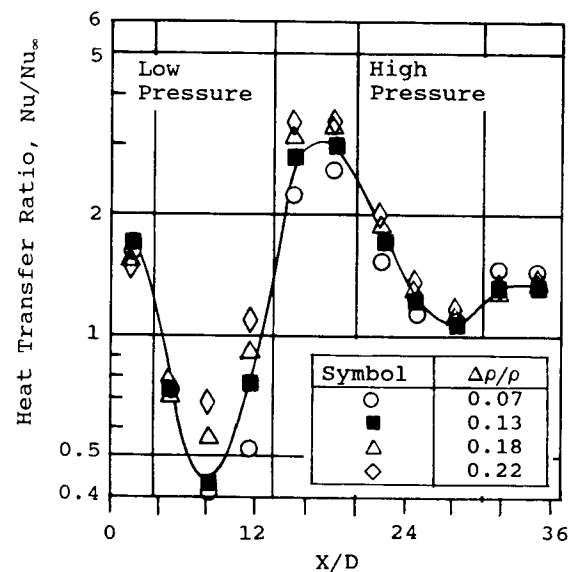 R_O=0.24, R/D=49

Fig. 6b   Effect of Wall-to-Coolant Density
          Difference on Heat Transfer Ratio
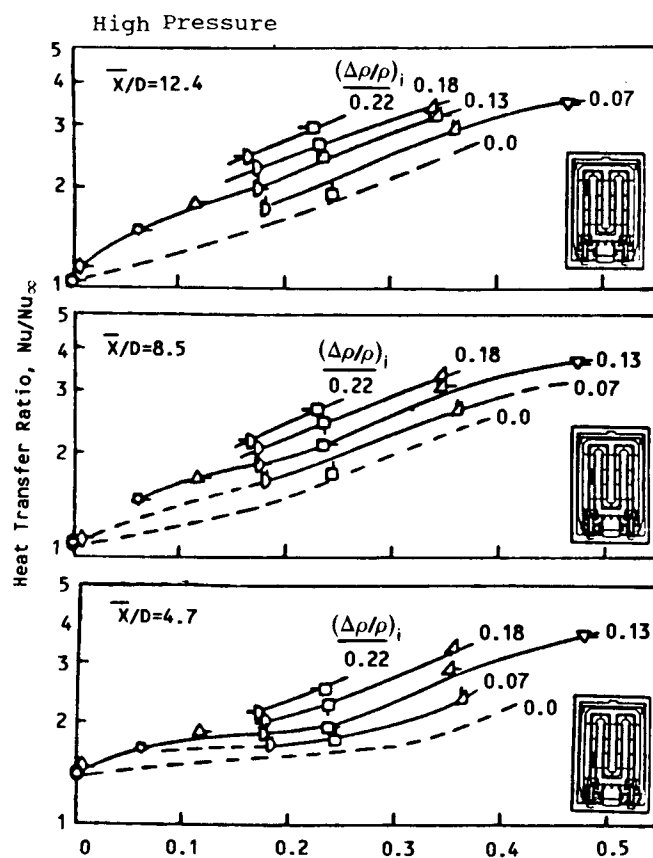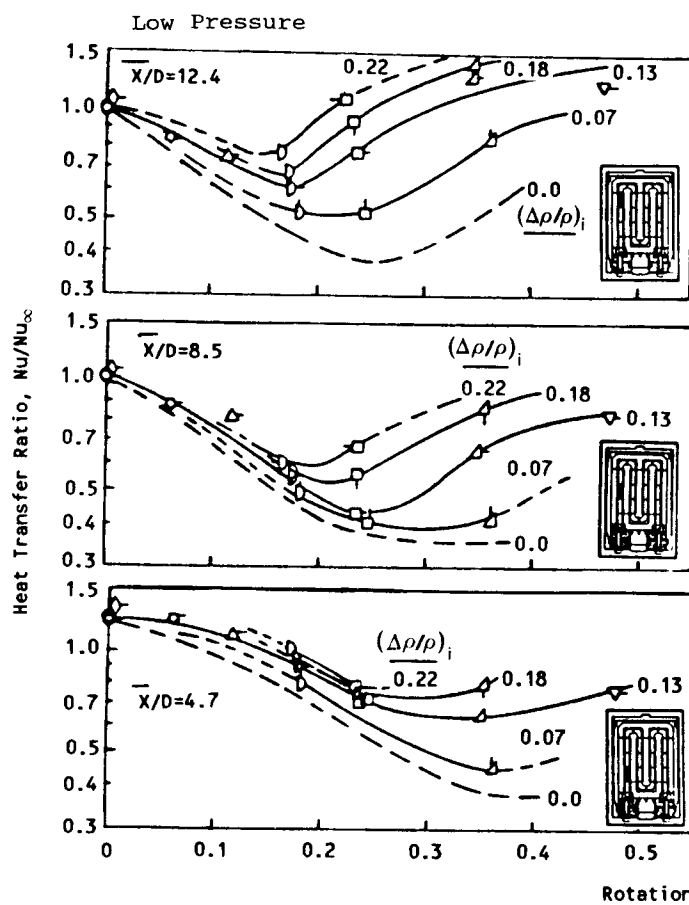   for Leading Surfaces; Re=25000,
          R_O=0.24, R/D=49

Fig. 7a   Effect of Rotation Number and Density Ratio on Heat Transfer Ratios in
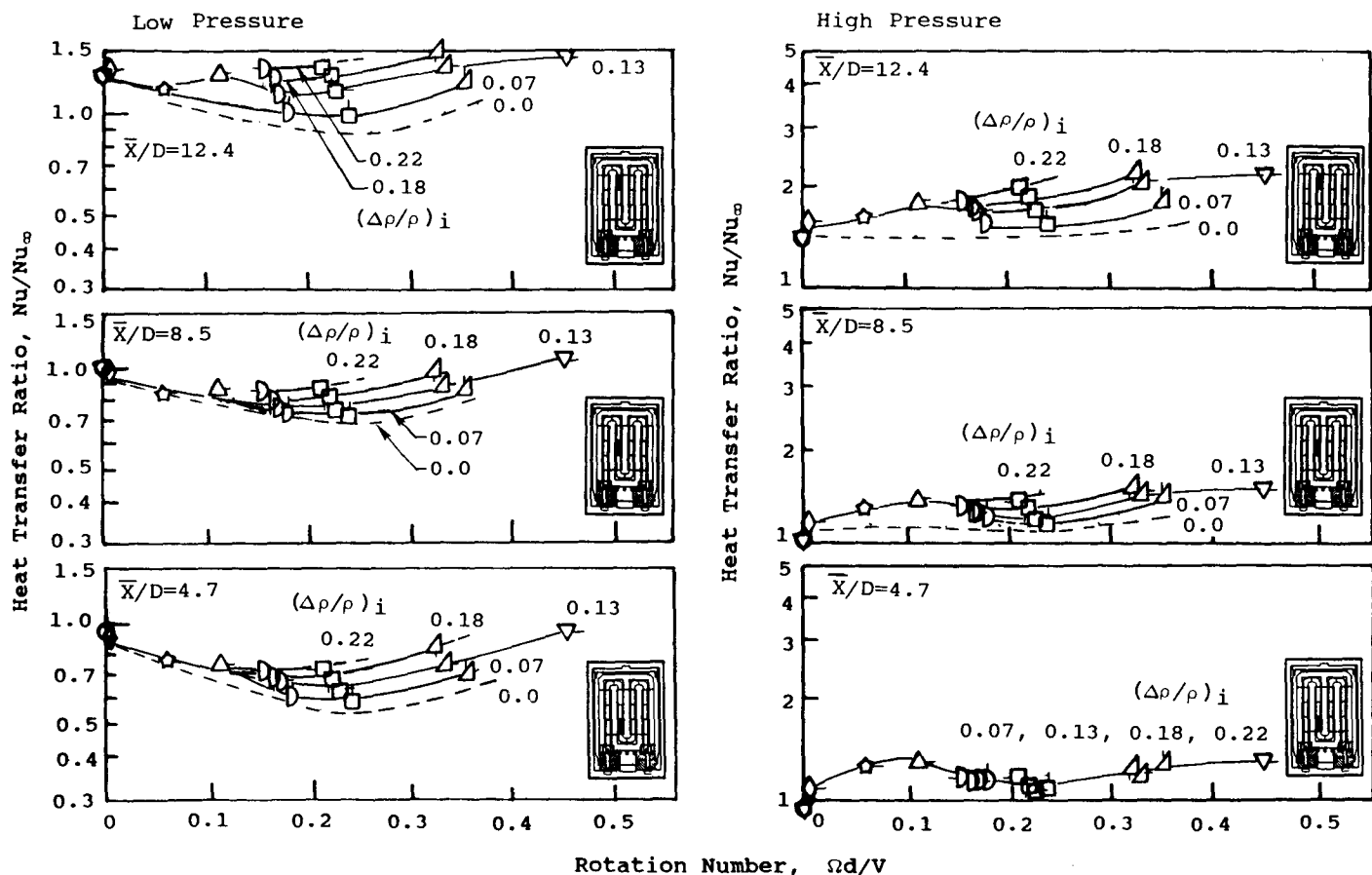   the First Passage; Re=25000, R/D=49

8

Fig. 7b Effect of Rotation Number and Density Ratio on Heat Transfer Ratios in
the Second Passage; Re=25000, R/D=49

effect of density ratio on the heat transfer ratio for a rotation number of 0 when film properties are used for the dimensionless heat transfer and flow parameters. Increasing the rotation number causes local increases in the heat transfer in the first passages by as much as 3.5 compared to the heat transfer for a rotation number of 0. Whereas, the heat transfer ratios for the high pressure surfaces increase sharply with increases in either the density ratio or the rotation number, with one exception, heat transfer in the second passage is relatively unaffected by variations of either parameter. The exception being near the inlet of the second passage, just downstream of the first turn. At this location the heat transfer increases slightly with increases in the rotation parameter and the density ratio. However, for larger x/D in the second passage the effect on the heat transfer for variations in rotation or density ratio diminishes.

Low Pressure Surfaces. The heat transfer from the low pressure surfaces from the first and second passages (Figure 7) is more complex than that from the high pressure surfaces. Heat transfer in the first passage decreases with increasing rotation number for low values of rotation number (i.e., $\Omega D/V < 0.2$ at the downstream location) and then subsequently increases again with increases in rotation for larger values of rotation number. Additionally, as with the high pressure surfaces in the first passage, heat transfer increases

with increases in the density ratio. A similar characteristic in the heat transfer distributions is observed in the second passage for radially inflow as well. However, with one exception, the large effects of density ratio observed on the low pressure surfaces of the first passage are diminished in the second passage. The exception is that heat transfer is slightly increased with increasing density ratio near the inlet of the second passage.

The more complicated heat transfer distributions on the low pressure surfaces of the coolant passages are attributed to 1) the combination of buoyancy forces and the stabilization of the near–wall flow for low values of the rotation number and 2) the developing, Coriolis driven secondary flow cells for the larger values of the rotation number. It is postulated that the relatively large effects from variations in density ratio near the inlet of the second passage and the small effects near the end of the second passage are due to the development of the near–wall thermal layers. Near the inlet of the second passage, the thermal layers are postulated to be thin because of the strong secondary flows in the first turn region. With increasing x/D, the turn dominated secondary flows diminish and the counteracting effect of buoyancy and the Coriolis generated secondary flow increases.

9

CORRELATING PARAMETERS

The analysis of the equations of motion for flow in rotating radial passages by Suo (1980), discussed above, showed that 1) the cross–stream flows will be proportional to the rotation number, $\Omega D/V$, and 2) the buoyant flows will be proportional to the buoyancy parameter, $(\Delta\rho/\rho)\,(R/D)(\Omega D/V)^2$.

The combined effect of the cross–stream flows and the buoyant flows is not easily ascertained from the equations of motion. The preceding discussions indicate that the combined effects are quite complex and are a strong function of flow direction. Therefore, the flow direction is also considered in the following paragraphs.

The buoyancy parameter defined above is equivalent to the ratio of the Grashof number (with a rotational gravitation term, $R\Omega^2$) to the square of the Reynolds number and has previously been used to characterize the relative importance of free– and forced–convection in the analysis of stationary mixed–convection heat transfer. Guidez (1988) used a similar analysis to establish appropriate flow parameters for the presentation of his results. These parameters, $\Omega D/V$ and $(\Delta\rho/\rho)\,(R/D)(\Omega D/V)^2$, will also be used in the present discussion of the effects of Coriolis and buoyancy forces on the heat transfer for inward and outward flow directions.

The data was analyzed to determine the effects of flow direction (radially inward or radially outward) on the heat transfer characteristics and to determine the differences between the first passage with outward flow downstream of an inlet, the second passage with inward flow downstream of a 180° turn and the third passage with outward flow downstream of a 180° turn. The variations of heat transfer ratio with buoyancy parameter for the heated surface at the most downstream location from the inlet or a turn for each of the three passages are shown in Figure 8. This is the streamwise location for each passage where heat transfer for stationary test conditions asymptotically approached the value of heat transfer for turbulent, fully developed flow.

The data presented in Figure 7 showed that the effects of Coriolis and buoyancy forces are coupled in the first two passages through the entire operating range investigated. The results from Figure 7 plus additional results from the third passage are combined with those for R/D = 33 and are presented in Figure 8 as the variation of the heat transfer ratio with the buoyancy parameter based on the local density ratio and radius, R. Thus, the range of the buoyancy parameter decreases with increasing values of x/D (i.e. decreasing temperature difference with increasing x). The ranges of heat transfer ratio for the last location in the first passage is shown as a shaded band with the results from the second and third passages for comparison.
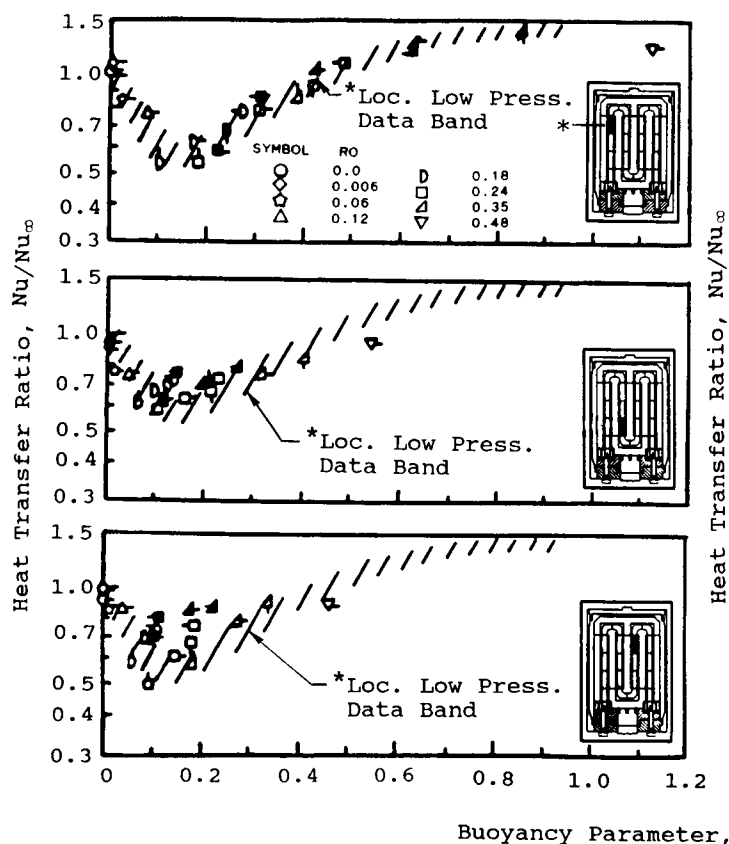

Fig. 8a   Comparison of Heat Transfer Ratios From the Low Pressure Surfaces of the First, Second and Third Passages
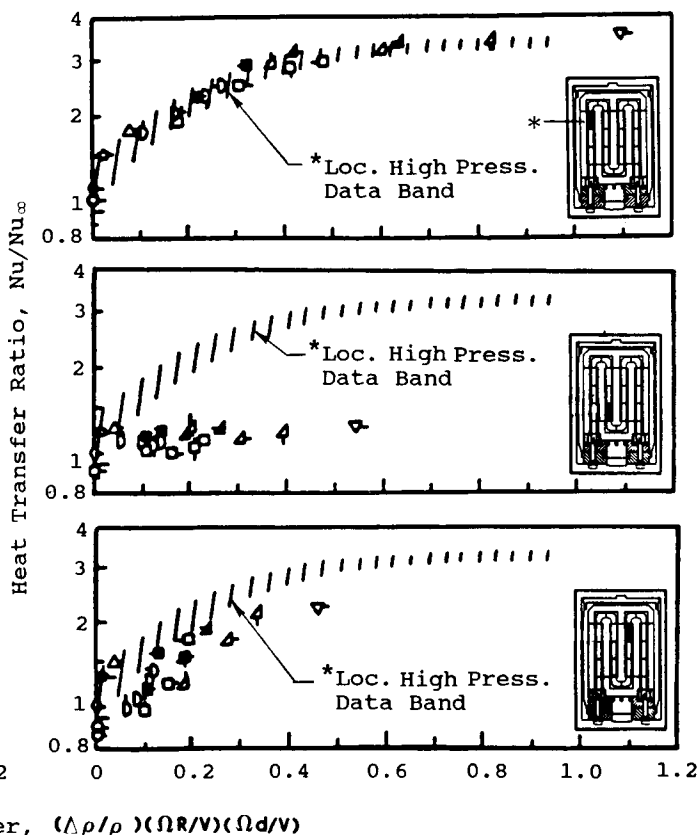
Fig. 8b   Comparison of Heat Transfer Ratios From the High Pressure Surfaces of the First, Second and Third Passages

ratio for the last location in the first passage is shown as a shaded band with the results from the second and third passages for comparison.

Heat transfer distributions from the low pressure surfaces of each of the three passages exhibit a similar relationship with the buoyancy parameter. Heat transfer decreases with increasing values of buoyancy between 0.0 and 0.15. Heat transfer subsequently increases again with increasing values of buoyancy. Heat transfer on the low pressure surfaces of rotating coolant passages is governed by complex relationships of streamwise location, rotation number and buoyancy parameter. However, the heat transfer results are reasonably well correlated in the first two passages by the buoyancy parameter for values of buoyancy parameter greater that 0.2.

The heat transfer results from the high pressure surfaces in the first passage are correlated well by the buoyancy parameter. The second passage with radially inward flow had different heat transfer characteristics than the first and third passages with radially outward flow. Whereas the heat transfer ratios for the high pressure surfaces of the first and third passages increased with the buoyancy parameter, the heat transfer in the second passage was lower and relatively independent of buoyancy parameter for values of buoyancy greater than 0.05. These results for co–flowing and counter–flowing buoyancy effects on the high pressure surfaces are generally consistent with the stationary combined free– and forced–convection experiments of Eckert et al. (1953). They measured decreased levels of heat transfer for the co–flowing condition (i.e. similar to that of radially inward flow in rotating systems). A more comprehensive comparison with of Eckert's results is presented in the next section.

COMPARISON WITH PREVIOUS STATIONARY EXPERIMENTAL RESULTS

Thus far this study has shown that rotational forces strongly influence turbulent heat transfer in rotating smooth passages for conditions found in gas turbine blades. However, variations in heat

transfer caused by rotation have been shown to be less for radially inward flowing passages than for radially outward flowing passages. These effects of flow direction in the present rotating heat transfer experiments are compatible with stationary heat transfer experiments conducted by Eckert et al. (1953). Three experiments were conducted in a large vertical circular tube (stationary) where they examined mixed–, free– and forced–convection heat transfer. These results are plotted as Nu_x vs. Gr_x in Figures 9 and 10. A free–convection limit consisting of a curve fit through the results of Eckert's free–convection experiment is shown in each figure. Circumferentially averaged results from the present rotating heat transfer experiment are shown as the symbols in Figures 9 and 10. Heat transfer data shown with the same symbol are for the same rotation number at three wall–to–coolant temperature differences.

The heat transfer results from the radially outward flowing passage from the present work are compared to results from the 1953 counter–flow experiments in Figure 9. For the stationary counter–flow experiments the wall thermal boundary layer, under gravity induced buoyancy forces, moves in a direction opposite to the mainstream flow. This is analogous, in a buoyant sense, to the rotating conditions with the radially outward flowing passage where the buoyancy force is induced by rotation and toward the axis of rotation. The averaged heat transfer data measured in the present experiments agrees remarkably well with Eckert's. The increasing slope through the data indicates the flow is in the mixed flow regime and buoyancy influences the circumferentially averaged heat transfer. For large values of Gr_x, heat transfer rates approach the free convection limit as established by Eckert. The data also indicates a higher free convection limit at the lower values of Gr_x. Eckert also noticed this trend when he compared the extreme forced–convection data at high Grashof numbers with the free convection data. For low values of Gr_x, forced convection dominates the heat transfer. As can be seen in the figure, the forced convection limit was not reached with the present set of experiments.
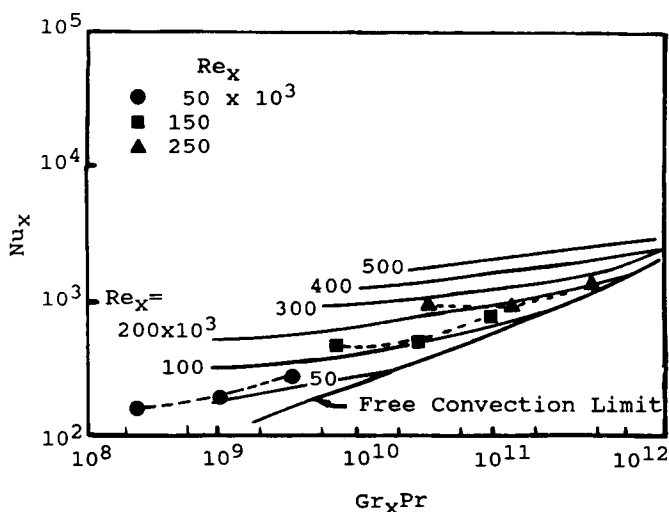
Fig. 9   Comparison of Circumferentially Averaged Heat Transfer Results for the First Passage with Stationary, Counterflow Heat Transfer Results (Eckert et. al.)(1953)
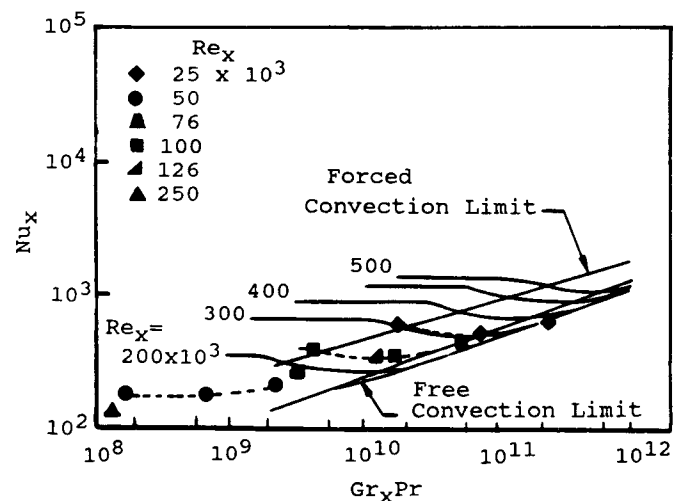

Fig. 10   Comparison of Circumferentially Averaged Heat Transfer Results for the Second Passage with Stationary, Parallel Heat Transfer Results (Eckert et. al.) (1953)

Shown in Figure 10 are the present heat transfer results from the radially inward flowing passage with the curve–fit results from Eckert. For this flow condition the buoyancy force and flow direction are coincident. Again, the present, average heat transfer results agree very well with those of Eckert. These results show that when the buoyancy acts in the same direction as the turbulent mainstream, heat transfer is inhibited in the mixed–convection regime. Both Eckert's results from stationary experiments and the present results from experiments with rotation show a local decrease in heat transfer for values of Gr_xPr in this mixed convection region. This local decrease is particularly important when these heat transfer results are compared with those from the counterflow experiments. When Nusselt numbers for similar flow conditions for the radially outward and inward flowing cases are compared, the counterflow (radially outflow) heat transfer is almost 70 percent greater than the corresponding parallel flow heat transfer (e.g. $Nu_x=875$ compared to 520). Eckert noted that the counterflow situation could result in heat transfer levels as much as twice those in the parallel flow case. This is especially significant when these results are circumferential averages of heat transfer around the perimeter of the coolant passage. As shown in previous discussion, local heat transfer rates can be significantly higher and lower than the circumferential averages.

CONCLUDING COMMENTS

This paper has presented an extensive body of experimental data from heat transfer experiments in a rotating square passage with smooth walls. The analysis of these experimental results to determine the separate effects of forced convection, Coriolis, buoyancy and flow direction on the heat transfer has resulted in the following observations and conclusions:

1. Density ratio and rotation number were found to cause large changes in heat transfer for radially outward flow and relatively small changes for radially inward flow.

2. The heat transfer ratio was found to be primarily a function of a buoyancy parameter on the low pressure surfaces of the coolant passages, regardless of flow direction.

3. The heat transfer ratio on the high pressure surfaces was significantly affected by flow direction. The heat transfer was found to be a strong function of a buoyancy parameter for the high pressure surfaces for radially outward flow. Whereas, the heat transfer was relatively unaffected by a buoyancy parameter for the radially inward flowing high pressure surface.

4. Increasing the density ratio generally caused an increase in heat transfer. However, the increase in heat transfer for the inward flowing passage was considerably less than that for outward flow.

5. Circumferentially averaged heat transfer results compared favorably with a previous stationary parallel and counterflow mixed–convection heat transfer experiment by Eckert et al. (1953). Heat transfer from the radially outward flowing passages compared with Eckert's counterflow case while the radially inward flowing results compared with Eckert's parallel flow case.

REFERENCES

Aladyev, I. T., 1954, "Experimental Determination of Local and Mean Coefficients of Heat Transfer for Turbulent Flow in Pipes," NACA TN 1356. (Translation from Russian.)

Boelter, L. M. K., Young, G. and Iverson, H. W., 1948, NACA TN 1451, Washington.

Brundrett, E. and Burroughs, P. R., 1967, "The Temperature Inner–Law and Heat Transfer for Turbulent Air Flow in a Vertical Square Duct," Int. J. Heat Mass Transfer, Vol. 10, pp. 1133–1142 .

Clifford, R.J., 1985, "Rotating Heat Transfer Investigations on a Multipass Cooling Geometry" AGARD Conference Proceedings No. 390: Heat Transfer and Cooling in Gas Turbines, May 6–10.

Eckert, E. R. G., Diaguila, A. J. and Curren, A. N., 1953, "Experiments on Mixed–, Free– and Forced–Convective Heat Transfer Connected with Turbulent Flow Through a Short Tube," NACA Technical Note 2974.

Guidez, J., 1988, "Study of the Convective Heat Transfer in Rotating Coolant Channel," ASME Preprint 88–GT–33 presented in Amsterdam, The Netherlands.

Han, J. C., Park, J. S. and Lei, C. K, 1984, "Heat Transfer and Pressure Drop in Blade Cooling Channels With Turbulence Promoters," NASA Contractor Report 3837.

Hart, J. E., 1971, "Instability and Secondary Motion in a Rotating Channel Flow," J. Fluid Mech., Vol. 45, Part 2, pp. 341–351.

Iskakov, K. M. and Trushin, V. A., 1983, "Influence of Rotation on Heat Transfer in a Turbine–Blade Radial Slot Channel," Izvestiya VUZ. Aviatsionnaya Tekhnika, Vol. 26, No. 1, pp. 97–99.

Johnson, B. V., 1978, "Heat Transfer Experiments in Rotating Radial Passages with Supercritical Water," ASME Heat Transfer (Bound proceedings from 1978 ASME Winter Annual Meeting).

Johnston, J. P., Halleen, R. M. and Lezius, D. K., 1972, "Effects of Spanwise Rotation on the Structure of Two–Dimensional Fully Developed Turbulent Channel Flow," J. Fluid Mech., Vol. 56, Part 3, pp. 533–557.

Kays, W. M. and Perkins, H. C., 1973, "Forced Convection, Internal Fow in Ducts." From Handbook of Heat Transfer, ed. by Rohsenow, W. M. and Hartnett, J. P., McGraw Hill, pp. 7–28 and 7–33.

Lokai, V. I. and Gunchenko, E. I., 1979, "Heat Transfer Over the Initial Section of Turbine Blade Cooling Channels Under Conditions of Rotation," Therm. Enging., Vol. 26, pp. 93–95.

Metais, B. and Eckert, E. R. G., 1964, "Forced, Mixed, and Free Convection Regimes," J. Heat Transfer, Vol. 64, pp. 295–296.

Moore, J., 1967, "Effects of Coriolis on Turbulent Flow in Rotating Rectangular Channels," M.I.T. Gas Turbine Laboratory Report No. 89.

Mori, Y., Fukada, T. and Nakayama, W., 1971, "Convective Heat Transfer in a Rotating Radial Circular Pipe (2nd Report)," Int. J. Heat Mass Transfer, Vol. 14, pp. 1807–1824.

Morris, W. D. and Ayhan, T., 1979, "Observations on the Influence of Rotation on Heat Transfer in the Coolant Channels of Gas Turbine Rotor Blades," Proc. Instn. Mech. Engrs., Vol. 193, pp. 303–311.

Morris, W., 1981, "Heat Transfer and Fluid Flow in Rotating Coolant Channels," Research Studies Press.

Rothe, P. H. and Johnston, J. P., 1979, "Free Shear Layer Behavior in Rotating Systems," J. Fluids Enging., Vol. 101, pp. 117–120.

Suo, M., 1980, Unpublished Notes, United Technologies Research Center.

Wagner, J. H., Johnson, B. V. and Hajek, T. J., 1989, "Heat Transfer in Rotating Passages with Smooth Walls and Radial Outward Flow," ASME Paper No. 89–GT–272.

Wagner, R. E. and Velkoff, H. R., 1972, "Measurements of Secondary Flows in a Rotating Duct," J. Eng. for Power, ASME Paper 72-GT-17.

Yang, J. W. and Liao, N., 1973, "An Experimental Study of Turbulent Heat Transfer in Converging Rectangular Ducts," Paper No. 73–WA/HT–27. ASME Journal of Heat Transfer.